ISSN: 1813-4890

Corrosion Mechanism of L316 Stainless Steel in Methanol Recovery Towers of Gas Fields

Hankezi Yisilamujiang [1], Mingyao Kou [2], Shiqi Liu [2], Qishu Zhou [1], Rongyao Zhang [2]

[1]Institute of Petroleum Engineering, Xi' an Shiyou University, Shaanxi Key Laboratory of Advanced Stimulation Technology for Oil & Gas Reservoirs, Shaanxi 710065, China;

[2] The Second Gas Production Plant, Changqing Oil Field, CNPC, Shaanxi 718500, China.

Abstract

To investigate the corrosion resistance of L316 stainless steel in methanol recovery towers, this study employed on-site weight-loss testing to measure corrosion rates, complemented by scanning electron microscopy (SEM), energy-dispersive X-ray spectroscopy (EDS), and 3D profilometry to analyze morphological characteristics of corrosion coupons. Results indicate that L316 exhibits general corrosion with concurrent pitting issues in the tower environment. Uniform corrosion rates in the upper and lower sections of the distillation column are quantified at 0.0004 mm/a and 0.0007 mm/a, respectively, primarily attributed to high chloride-ion concentration and high-temperature conditions.

Keywords

L316 stainless steel; gas field produced water; methanol recovery tower; corrosion mechanisms.

1. Introduction

The treatment method for reinjecting produced water from gas fields is an important approach to reducing environmental pollution and enhancing the economic efficiency of oilfield development during gas field operations [1-2]. The produced water treatment system in a certain gas field in northern Shaanxi employs a multi-stage process to remove oil, solid impurities, iron ions, and other contaminants from the produced water. It also utilizes a methanol recovery unit to recycle methanol, thereby enabling its reuse. The process flow is illustrated in Figure 1. The methanol recovery tower separates methanol from the mixture by leveraging differences in the boiling points of its components. Through multi-stage countercurrent contact reflux driven by thermal energy and constrained by phase equilibrium, volatile methanol transitions from the liquid phase to the gas phase, while less volatile water moves in the opposite direction. This process continuously separates methanol and purifies the wastewater [3]. However, corrosion inside the methanol recovery tower has become a critical factor affecting equipment performance and service life.

This study investigates the corrosion mechanism of L316 material in the methanol recovery tower through corrosion coupon tests, analyzing the corrosion morphology and calculating the corrosion rate. The findings aim to provide a reference for future corrosion prevention measures.

ISSN: 1813-4890

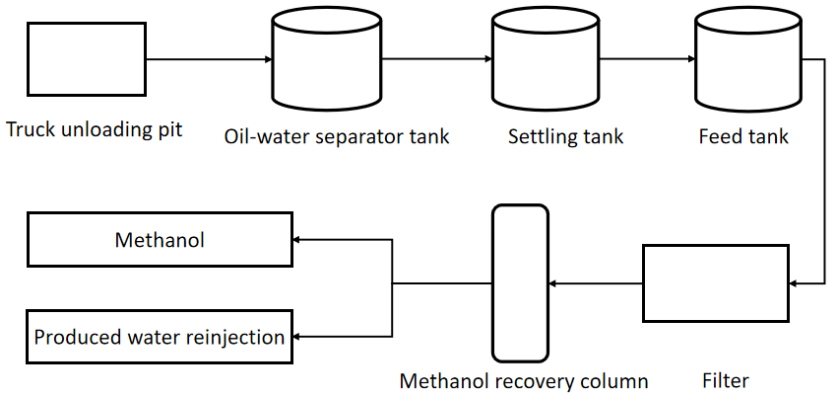

Fig. 1 Process flow diagram

2. Experimental method

2.1. Analysis of water quality of gas field produced water

Water quality analysis of the produced water was conducted in accordance with SY/T 5523-2016 "Analysis Methods for Oilfield Waters".

2.2. Determination method of corrosion rate

Coupons made of L316 stainless steel were suspended on the 10th tray of the lower section and the 38th tray of the upper section of the fractionating column. The internal structure of the tray column is shown in Figure 2. After a predetermined period, the coupons were retrieved. Their weights before and after corrosion were accurately measured in accordance with the relevant requirements of SY/T 0026—2024 "Corrosion Rate of Metallic Materials in Oil and Gas Field Media". The corrosion rate was then calculated based on the weight-loss method.

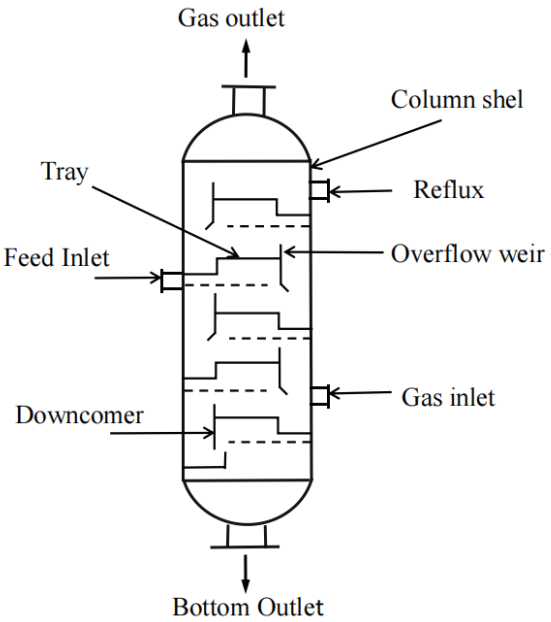

Fig. 2 Internal structure diagram of tray column

2.3. Analysis Methods for Corrosion Coupon Morphology

Through SEM and EDS analysis of the surface of the corroded coupons, as well as 3D profiling system analysis, the depth of pitting corrosion on the coupon surface after the removal of corrosion products was measured to assess the corrosion conditions.

ISSN: 1813-4890

3. Result and discussion

3.1. Produced water quality analysis

The water quality analysis of the produced water is shown in table 1.

Table 1 Water quality analysis results

Parameter	29 April	3 May	5 July
pH	6.31	6.95	6.32
SS (mg/L)	530	215	652
Cl^- (mg/L)	18875	16047	25961
HCO_3^- (mg/L)	303	271	172
SO_4^{2-} (mg/L)	70	103	65
Total Iron (mg/L)	19	29	98
Ca^{2+} (mg/L)	8978	7292	4833
Mg^{2+} (mg/L)	353	391	486
Ba^{2+} (mg/L)	252	313	461
Sr^{2+} (mg/L)	139	202	450
$\Sigma Na^+ + K^+$ (mg/L)	1246	1242	13430
TDS (mg/L)	30235	25891	45956
Oil (mg/L)	1457	972	1815
Methanol Content (%)	42	42	42
Water Type	$CaCl_2$	$CaCl_2$	$CaCl_2$

As can be seen from Table 1, the produced water is classified as the calcium chloride ($CaCl_2$) type. The high chloride ion content suggests a potential risk of pitting corrosion. Additionally, the total dissolved solids (TDS) are generally elevated, with high and variable concentrations of scale-forming cations, indicating a pronounced tendency for scaling.

3.2. Corrosion rate measurement results

Corrosion coupons in the fractionating column are shown in Figure 3, and the corrosion rates are presented in Figure 4.

(a) The 10th Tray (b) The 38th Tray

Fig. 3 Corrosion Coupons Located in the Fractionating Column

ISSN: 1813-4890

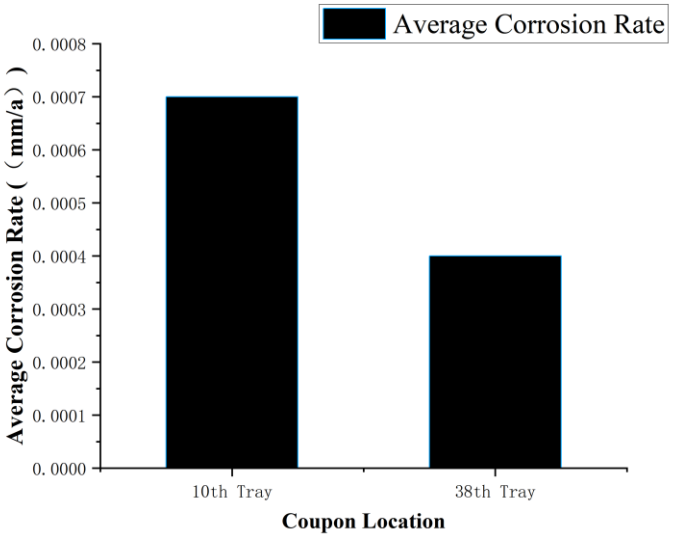

Fig. 4 Corrosion Rate Results of L316 Coupons

As can be seen from Figure 4, the corrosion at the bottom of the column is more severe than that at the top. However, the uniform corrosion rates at both locations are below 0.025 mm/a, which is classified as mild corrosion.

3.3. Microscopic Morphology and Elemental Composition of the Corrosion Product Film

SEM and EDS analyses were conducted on the surface of the coupon, with the results presented in Figure 5 and Figure 6, respectively. The surface of the coupon was observed to be rough and irregular, characterized by significant corrosion features, granular structures, as well as micro-cracks and pores.

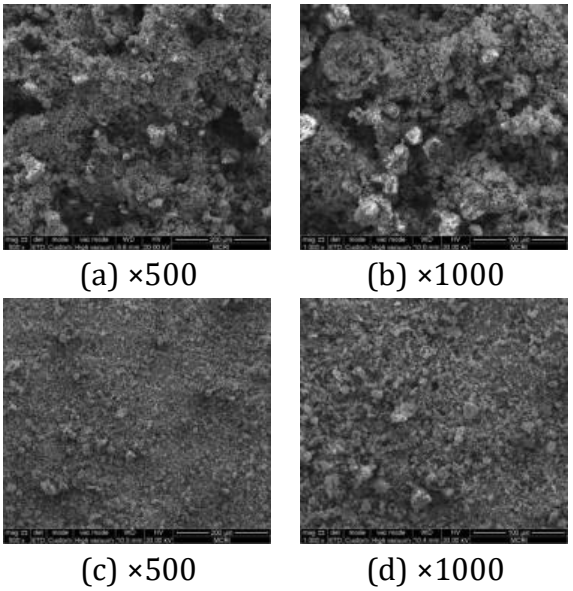

Fig. 5 SEM images of corrosion coupons: (a)(b) the 10th tray; (c)(d) the 38th tray

ISSN: 1813-4890

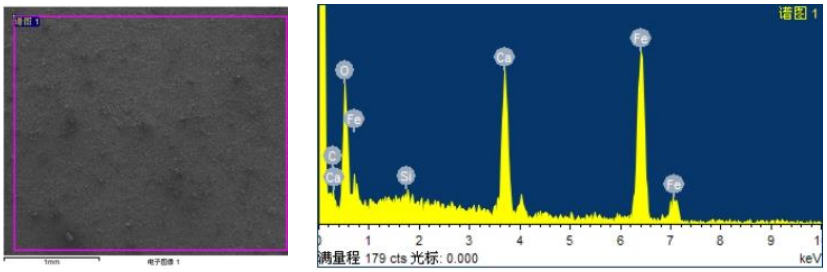

coupon from the upper tray

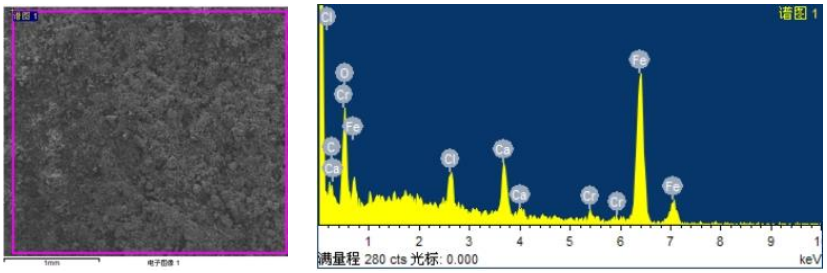

coupon from the lower tray

Fig. 6 EDS analysis of corrosion coupons from the upper and lower trays

The results of EDS elemental analysis are presented in Table 2. The surface composition of the coupons was similar, primarily consisting of C, O, Ca and Fe. This is mainly attributed to the fact that the coupon surfaces were covered with scale.

Table 2 Energy spectrum analysis results

Element	Upper layer		Lower layer	
	Wt.%	At.%	Wt.%	At.%
C K	10.48	25.03	3.37	9.82
O K	20.68	37.41	17.15	37.68
Si K	0.53	0.54	-	-
Cl K	-	-	3.1	2.97
Ca K	8.33	6.07	4.43	3.89
Cr K	-	-	1.52	1.07
Fe K	59.98	30.95	70.43	44.57
Total	100	100	100	100

Pitting corrosion was observed on the L316 stainless steel coupon from the lower section of the fractionating column. The morphology of the pits was analyzed using a 3D profiling system, and the results are shown in Figure 7. The maximum pit depth on the L316 coupon was 70 μm, with a pitting rate of 0.544 mm/a.

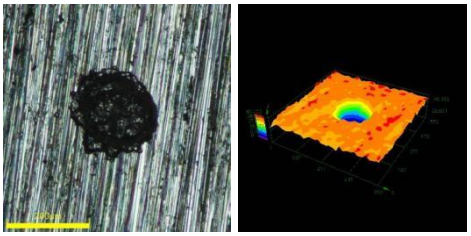

Fig. 7 Pitting morphology on the corrosion coupon from the lower tray

ISSN: 1813-4890

4. Corrosion mechanism analysis

L316 stainless steel is an austenitic stainless steel with a typical chemical composition range of chromium (16%–18%), nickel (10%–14%), and molybdenum (2%–3%). The synergistic effect of these elements enables the formation of a stable passive film in oxidizing media. This film effectively blocks the erosion by corrosive substances, reduces the electrochemical corrosion rate, and plays a crucial role in corrosion protection [4-5]. The corrosion mechanism of L316 stainless steel in the methanol recovery tower can be attributed to the following factors:

The produced water from the gas field has a relatively low pH, consistently below 7.0. In this acidic environment, the passive film on the surface of L316 stainless steel is compromised by the acidic medium, accelerating metal dissolution reactions and readily leading to uniform corrosion [6].

The produced water contains a high concentration of Cl^-, exceeding 15,000 mg/L. EDS analysis results indicate the presence of Cl^- on the coupon from the lower tray, while it was not detected on the upper tray coupon. Consequently, pitting corrosion occurs on the lower tray and is more severe than uniform corrosion. Cl^- is a highly aggressive ion that adsorbs onto the stainless steel surface, dissolves the passive film by forming $CrCl_3$, and thereby destroys it, initiating pitting corrosion. When the mass concentration of Cl^- exceeds 0.5 g/L, stainless steel becomes susceptible to pitting and crevice corrosion [7-8]. Furthermore, higher Cl^- content in the corrosive medium lowers the critical pitting temperature (CPT) of L316 stainless steel, increasing the risk of pitting corrosion [9].

The produced water contains high and fluctuating concentrations of scale-forming cations (e.g., Ca^{2+}, Mg^{2+}, Ba^{2+}, Sr^{2+}), which readily lead to the formation of carbonate and sulfate scales. These deposits exacerbate corrosion. The formation of scale not only reduces heat exchange efficiency but can also initiate under-deposit corrosion.

The operating temperature of the methanol recovery tower is generally elevated. High temperatures lower the pH of the produced water, increase the kinetic energy of molecules and ions, alter chloride ion activity, and thereby accelerate the corrosion rate [10]. High-temperature conditions also degrade the protective quality of the oxide film; the grain size and intergranular spaces within the oxide film may increase, compromising its protective function on the base metal [11].

5. Summary

The produced water from a gas field in northern Shaanxi is generally acidic, characterized by low pH, high levels of total dissolved solids (TDS), suspended solids, and chloride ions, indicating a significant corrosion risk.

Field corrosion testing of L316 stainless steel coupons in the tray column revealed both uniform corrosion and pitting corrosion, with pitting corrosion being the more severe issue.

The high chloride ion content and elevated temperature are identified as the primary causes of corrosion in L316 stainless steel. Moreover, these two factors exhibit a synergistic effect that accelerates the corrosion rate. Therefore, corresponding mitigation strategies targeting these factors should be implemented in the future to reduce corrosion

References

[1] Zhang Shihu, Wei Keying, Wang Wei, et al. Study on the optimization of produced water treatment process in Sulige gas field [J]. Inner Mongolia Petrochemical, 2018, 44 (12) : 105-109.

[2] Yuan Bo, Guan Shuo, Ma Xiaohui. Disposal and Utilization of Produced Water from Oil and Gas Fields in USA [J]. Environmental Protection of Oil and Gas Fields, 2019, 29 (02) : 8-11 + 60.

ISSN: 1813-4890

[3] Sun Huachao, Wu Weiran, Zhu Dechun, et al. Evaluation of the effect of alcohol-containing wastewater treatment process in Daniudi gas field [J]. China Petroleum and Chemical Standards and Quality, 2017, 37 (06) : 120-121.

[4] Xian Kelong, Xiao Ying, Zhang Hailong, et al. In-situ preparation of corrosion-resistant sulfides on the surface of 316L stainless steel and its corrosion protection in different chlorine-containing media [J / OL].Surface technology, 1-27 [2025-06-19].

[5] Yu Xiaoyu, Ma Zhenqiang, Sun Kangrui, et al. Research on corrosion resistance of 316L stainless steel in H2SO4-CuSO4 solution [J]. Salt Science and Chemical Engineering, 2025,54 (08) : 13-16.

[6] Li Litao.Research on material selection and anti-corrosion technology of chemical wastewater treatment equipment [J]. Chemical safety and environment, 2025,38 (05) : 65-68.

[7] Wei Xin.Local corrosion behavior of passive metals in chloride environment [D]. Dalian University of Technology, 2013.

[8] Wang Yun.Electrochemical corrosion behavior and corrosion inhibition of different metals in hydrogen ion medium [D]. Northwest University, 2016.

[9] Liao Kexi, Cao Zenghui, He Zhanfeng. Effect of chloride ion on critical pitting temperature of 316L stainless steel [J]. Corrosion and protection, 2017,38 (06) : 446-448 + 455.

[10] Guo Jijiang, Wang Chao. Research on equipment corrosion protection and control strategy [J]. China Equipment Engineering, 2025, (14) : 8-10.

[11] Duan Zhengang, Du Donghai, Zhang Lefu, et al. High temperature electrochemical corrosion behavior of 304 and 316L stainless steels [J]. Journal of Shanghai Jiaotong University, 2016,50 (02) : 215-2.